Anisotropic Diffusion by a Recursive Linear Convolving Method : Application to Space-time Segmentation and Pattern Recognition

Santiago VENEGAS-MARTINEZ, Juan Manuel RENDON and Georges STAMON
Laboratory of Systèmes Intelligentes de Perception
UFR Mathématiques et Informatique, Université René Descartes, Paris V
45 rue des Saints Pères, 75006 Paris
Email : venegas@math-info.univ-paris5.fr, rendon@math-info.univ-paris5.fr, and
stamon@math-info.univ-paris5.fr
http://www.math-info.univ-paris5.fr/sip-lab

Abstract

This paper presents a recursive linear convolving method to performe anisotropic diffusion in images. The proposed method based on the linear filtering technique gives an useful evolving interface in boundary propagating. The novel approach is that there is not need to estimate local and global properties previously of the concerned propagating boundary, it making a fast algorithm. However these properties can be obtained directly from the evolving interface in our proposed method. Since the proposed method, formulated in the continuous space, can be implemented efficiently and with robustness in the discrete space, we propose practical applications like space-time segmentation and pattern recognition.

Keywords : isotropic diffusion, anisotropic diffusion, boundary propagating, segmentation, video sequence.

1. Introduction

It is well known that a simple way of modifying the linear scale-space paradigm represents an useful idea to solve isotropic diffusion problems. In this way, the importance of multiscale descriptions of images has been recognized. A clean formalism of scale-space filtering was introduced by Witkin [1], and further developed by Koenderink [2], Babaud [3], Yuille [4], and Hummel [5].

Traditionally, anisotropic diffusion has been formulated as a process that will mainly take place in the interior of regions, and it will not affect the region boundaries. It is intuitive that the success of the diffusion process is restricted by using a subclass of the monotonically decreasing functions [6].

Recently, anisotropic diffusion has been used to formulate propagating interfaces to design a general framework for modeling the evolution of boundaries. For that, the boundary value is formulated using initial value partial differential equations which describe interface motion.

Since the aim is to provide computational techniques for tracking moving interfaces. Initially deformable models « snakes » based on minimizing an energy along a curve were formulated [7]. A geometric alternative for the snake model was introduced in level set methods [8] in which an evolving curve was formulated. The method works on a fixed grid, usually the image pixels grid, and automatically handles changes in the topology of the evolving contour. The geodesic active contour model was born latter. It is both a geometric model as well as energy functional minimization. Although the geodesic active contour model has many advantages over the snake, its main drawback is its nonlinearity that results in inefficient implementations.

On the other hand, deformable models are used for the tasks of image segmentation, tracking of moving objects in video sequences [9][15], applications like $3D$ shape reconstruction in computer vision, applications in pattern recognition where each object can be described using a function named « descriptor of the region ».

In this work we introduce a recursive linear convolving method to perform anisotropic diffusion efficiently and with robustness in the discrete space. Consequently we provide a computational technique for tracking moving interfaces and any applications in computer vision.

This paper addresses the problem of simultaneously tracking non-rigid objects using a coupled front propagation model that integrates boundary–based and region based information.

This paper is organized as follows : Section 2 reminds the criteria for obtaining isotropic diffusion. In Section 3 we give a brief background on anisotropic diffusion and our recursive linear convolving method. In Section 4 we show the curve evolution as a profitable result of the recursive linear convolving method. In Section 5 and 6 we show the applications to space-time segmentation and pattern recognition respectively. Finally, in Section 7 the main conclusions of this work are shown.

2. Isotropic diffusion

The essential idea of this approach is quite simple : embed the original image in a family of derived images $I(x,y,t)$ obtained by convolving the original image $I_0(x,y)$ with a Gaussian kernel $G(x,y;t)$ of variance t :

$$I(x,y,t) = I_0(x,y) * G(x,y;t). \qquad (1)$$

Larger values of t, the scale-space parameter, correspond to images at coarser resolutions. See Fig. 1. As pointed out by Koenderink [2] and Hummel [5], this one parameter family of derived images may equivalently be viewed as the solution of the heat conduction, or diffusion, equation

$$\begin{cases} I_t = \Delta I = (I_{xx} + I_{yy}), \\ I(x,y,0) = I_0(x,y) \end{cases} \qquad (2)$$

where Δ indicates the Laplacian operator with respect to the space variables.

Also Marr and Hildreth [10] have studied previously Gaussian blurring and the natural boundaries of objects.

Koenderink motivates the diffusion equation formulation by stating two criteria.

1. *Causality :* Any feature at a coarse level of resolution is required to possess a (not necessarily unique) « cause » at a finer level of resolution although the reverse need not be true.
2. *Homogeneity and Isotropy :* The blurring is required to be space invariant.

In fact the goal of this paper is to replace the second criterion by something more useful.

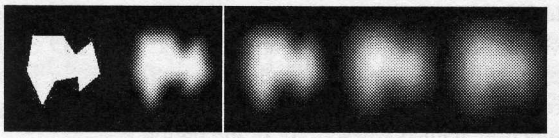

Figure 1 : *From left to right : A set of images 2-D* $I(x,y,t)$ *obtained by convolving the original one with Gaussian kernels* $t = 0,5,10,20,30$.

3. Anisotropic diffusion

Perona and Malik [6] have enunciated the criteria which they believe the anisotropic diffusion equation formulation must satisfy.

1. *Causality :* As pointed aout by Witkin and Koenderink, a scale-space representation should have the property that no spurious detail should be generated passing from finer to coarser scales.
2. *Immediate Localization :* At each resolution, the region boundaries should be sharp and coincide with the semantically meaningful boundaries at that resolution.
3. *Piecewise Smoothing :* At all scales, intraregion smoothing should occur preferentially over interregion smoothing.

In agreement with these criteria, now let us briefly review non-linear diffusion in image processing.

3.1 Classical definition

Perona and Malik have introduced the following diffusion equation

$$\begin{cases} I_t = div\left(g\left(|\nabla I|\right)\nabla I\right), \\ I(x,y,0) = I_0(x,y) \end{cases} \qquad (3)$$

where ∇ indicates the gradient operator with respect to the space variables, div indicates the divergence operator, and function g is an « edge-sttoping » function, for example,

$$g\left(|\nabla I|\right) = e^{-(|\nabla I|/k)^2} \qquad (4)$$

or, similarly

$$g\left(|\nabla I|\right) = 1/(1 + (|\nabla I|/k)^2). \qquad (5)$$

Equation (3) can be presented in form

$$I_t = g(x,y,t)\Delta I + \nabla g \cdot \nabla I. \qquad (6)$$

If $g(x,y,t)$ is a constant then (6) reduces to the isotropic heat diffusion equation $I_t = g\Delta I$, hence the diffusion coefficient g is assumed to be a constant independent of the space location.

In the diffusion equation framework of looking at scale-space, the first idea to solve isotropic diffusion problems are gived by the general expression in form

$$\begin{cases} I_t = |\nabla I| g\left(div\left(\nabla I/|\nabla I|\right), t\right). \\ I(x,y,0) = I_0(x,y) \end{cases} \qquad (7)$$

In the particular case if g is equal to +1 or –1 then equation (7) corresponds to basic morphological operators : dilatation and erosion using a ballon like an elementary structure.

On the other case, if function $g(s,t) = t \cdot s$ then equation (7) will be performed by

$$\begin{cases} I_t = t|\nabla I| div\left(\nabla I/|\nabla I|\right). \\ I(x,y,0) = I_0(x,y) \end{cases} \qquad (8)$$

This equation, similar to Sethian and Osher [8] approximation, corresponds to anisotropic diffusion in the level set direction. Also this equation has been studied in detail previously by Gage and Hamilton [11].

Since using descriptive definition of $g(s,t) = (t \cdot s)^{1/3}$ from axioms in Alvarez's works [12], equation (7) can be presented in form

$$\begin{cases} I_t = |\nabla I|\left(t \cdot div\left(\nabla I/|\nabla I|\right)\right)^{1/3}. \\ I(x,y,0) = I_0(x,y) \end{cases} \qquad (9)$$

This equation allows to perform anisotropic diffusion along level set direction.

After we have reviewed classical definitions of anisotropic diffusion of a general class of elliptic equations, now we shall present a recursive linear convolving method to perform anisotropic diffusion.

3.2. Our performed approximation

Instead of using edge detectors, an alternative approach of performing non-linear diffusion is adopted in the algorithms that are ables to adapt itself locally to the image by combining the smoothing capability of the linear averaging filter with the edge-preserving capability of the median filter.

In order to perform this task we propose a recursive linear convolving method that makes a systematic distinction between edges and homogeneous regions. The method is very simple : thresholding relatively, the output image will be composed with intensity values of the smoothed and non smoothed input image.

Our performed approximation is presented by

$$\begin{cases} I(x,y,t+1) = S(I(x,y,t) * G(x,y;k)) \\ I(x,y,0) = I_0(x,y) \end{cases}, \quad (10)$$

where $*$ indicates the convolving operator, $G(x,y;k)$ a kernel function, k the scale-space parameter. The operator S makes a systematic distinction between edges,

$$S(u(t)) = \begin{cases} u(t-1); & u(t) \geq h \\ u(t); & u(t) < h \end{cases}, \quad (11)$$

where h is the relative threshold computed in the neighboring points of (x,y). The blurring takes place separately in each region with no interaction between regions. Fig. 2 shows anisotropic diffusion.

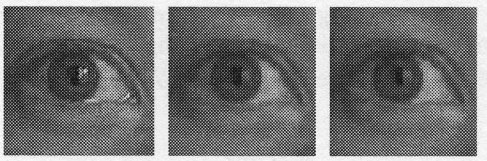

Figure 2 : *From left to right : Original image, classical, curvature flow, our performed approximation.*

Looking at the variation in time of the slope edges, we are interested in the particular case of the image $\Phi_0(x,y)$ defined as follows,

$$\begin{cases} +c & (x,y) \in \Omega_{in} \\ -c & (x,y) \in \Omega_{out} \end{cases}, \quad (12)$$

where c is a constant. The image domainis considered to be made up of two parts : the foreground part, noted Ω_{in}, and the background part noted Ω_{out}.

Our performed approximation simplifies to

$$\begin{cases} \Phi(x,y,t+1) = S(\Phi(x,y,t) * G(x,y;k)) \\ \Phi(x,y,0) = \Phi_0(x,y) \end{cases}, \quad (13)$$

where operator S simplifies to

$$S(u(t)) = \begin{cases} u(t-1); & u(t) \geq 0 \\ u(t); & u(t) < 0 \end{cases}. \quad (14)$$

In this way, Fig. 3 shows any examples of isotropic and anisotropic diffusion using expressions (2), (8), (13).

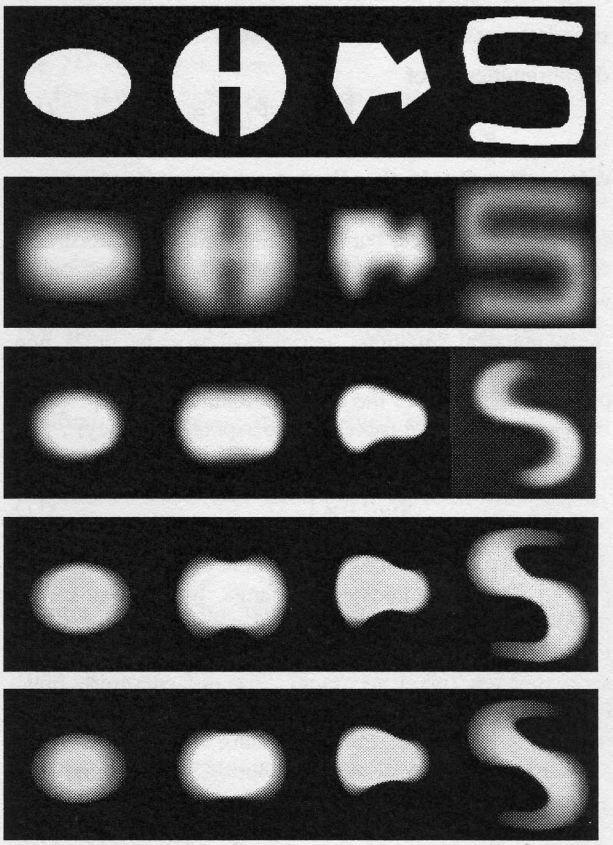

Figure 3 : *From top to bottom : original image, isotropic diffusion, anisotropic diffusion, anisotropic diffusion using a Gaussian function, and anisotropic diffusion using a median filter.*

Since performed approximation is based on linear convolving method, the expression (13) can be very easily extended to higher dimensions, like to perform anisotropic diffusion in the three dimensional space,

$$\begin{cases} \Phi(x,y,z,t+1) = S(\Phi(x,y,z,t) * G(x,y,z;k)) \\ \Phi(x,y,z,0) = \Phi_0(x,y,z) \end{cases}. \quad (15)$$

The continuous space can be implemented efficiently and with robustness in the discrete space.

4. Curve evolution

Enjoying the well known idea of using an image $\Phi^{t}_{(x,y)}$ as the auxiliary function allowing efficient numerical schemes, we will show curve evolution in our performed approximation.

The crossing by zero sets of the images $\Phi^{0}_{(x,y)}, \Phi^{1}_{(x,y)}, \Phi^{2}_{(x,y)}, \ldots$ are respectively the curves noted $\Gamma^{0}_{(x,y)}, \Gamma^{1}_{(x,y)}, \Gamma^{2}_{(x,y)}, \ldots$ that defines the boundary between the two domains Ω_{in} and Ω_{out}, such that $\Gamma^{t}_{(x,y)}$ is the discontinuities set of

$$\Phi : \Gamma^{t}_{(x,y)} = \left\{(x,y) / \Phi^{t}_{(x,y)} = 0\right\}. \tag{16}$$

4.1 Performing in the discrete space

In the discrete space, curve position (sub-pixel accuracy) can be computed by interpoling in the neighboring points where intensity values of $\Phi^{t}_{(x,y)}$ change de sign.

In practical situations, curve evolution becomes non useful because is a slow process. In order to accelerate this process and to reduce the computational cost, we propose, in the discrete space (pixel or super-pixel accuracy) , that operator S becomes

$$S(u(t)) = \begin{cases} +c; & u(t) \geq 0 \\ -c; & u(t) < 0 \end{cases}. \tag{17}$$

The operator S makes a systematic distinction between points becoming candidates to change. In this way kernel function G represents the weighted contributions of pixels to compute the speed mesure. Using this numerical approximation (pixel accuracy) for the curvature flow, Fig. 4 shows any curves evolving in a Euclidean plane by its curvature and vanishes at a point, the propertie well studied in the theory of curve evolution. In the same way as the level set theory, there is a curve noted $\Gamma^{0}_{(x,y)}$ that generates the family of curves in expression (16) which are generated from the movement of the initial curve $\Gamma^{0}_{(x,y)}$ in the direction of its inward Euclidean normal vector

$$\mathbf{N} = \nabla\Phi / |\nabla\Phi|. \tag{18}$$

The speed of this movement is supposed to be a scalar function of the curve curvature

$$K = div\left(\nabla\Phi / |\nabla\Phi|\right). \tag{19}$$

The curve evolution produces the associated motion for the position vector (x, y). These positions are updated using the performed approximation scheme showed in section 3.2.

The evolution equation can be presented as

$$\frac{\partial\Phi(t)}{\partial t} = F|\nabla\Phi|. \tag{20}$$

where the force F is the weighted function derived by convolving the input image Φ with a kernel function G.

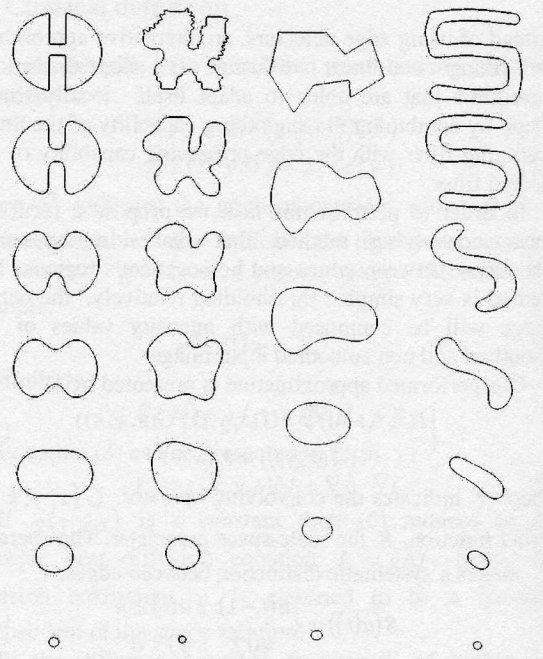

Figure 4 : *From top to bottom : curve evolutions* $\Gamma^{0}, \Gamma^{1}, \Gamma^{2}, \ldots$

The evolving model is capable to deal with topological changes of the moving front (proximity between two edges), merging and splitting are made by keeping constant $+h$ and $-h$ respectively in operator S , see Fig. 5.

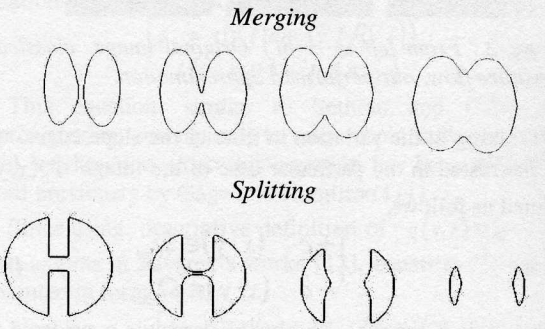

Figure 5 : *From left to right : curve evolutions* $\Gamma^{0}, \Gamma^{1}, \Gamma^{2}, \ldots$ *Top : merging, Bottom : splitting.*

On the other hand, the signed distance function computed in the fast marching method proposed by Osher and Sethian [13] is a computationally optimal numerical method. This method enjoys a computational complexity bound of $O(N \log N)$, where N is the number of grid points in the narrow band.

In our performed diffusion process the computational complexity is WN, where N is the number of grid points in the neighboring grid points of $\Gamma^t_{(x,y)}$, and W is the size of kernel function G.

Other proposed methods based in numerical approximation for the curvature flow becomes unstables. See in Fig. 6 a comparison with Kimel's approximation [14]. The two methods begin with a curve evolving by its curvature and vanishes at a point. One can see legs as the time step is increased.

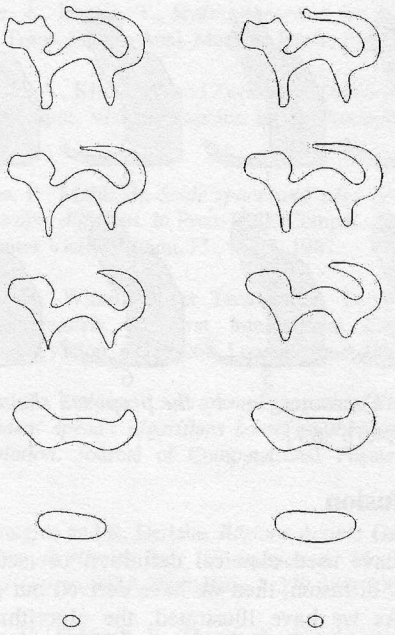

Figure 6 : *Curvature flow by the proposed scheme. Left : Rkimel's approximation, Right : our approximation.*

Taking crossing by zero sets in expression (15) we can easily extend to higher dimensions, like to follow fronts in the three dimensional space (surfaces) for the image $\Phi^{t}_{(x,y,z)}$ such that $\Gamma^t_{(x,y,z)}$ is the discontinuities set

$$\Phi : \Gamma^t_{(x,y,z)} = \{(x,y,z) / \Phi^t_{(x,y,z)} = 0\}. \qquad (21)$$

The continuous space can be implemented efficiently and with robustness in the discrete space.

5. Application to space-time segmentation

The introduced framework in section 3 is now applied to the segmentation of moving objects in a video sequence. Let I_n be the image number n of the sequence. We consider that each frame I_n can be divided into two regions : the background noted $\Omega_{n,out}$, and the moving object noted $\Omega_{n,in}$. Their common boundary is noted Γ_n. In this part of the work , we search for $\Omega_{n,out}$ and $\Omega_{n,in}$. Contour location in frame n is used as initial condition for the $2D$ solution in frame $n+1$.

For this, we will try to perform the motion equation

$$\frac{d\Phi}{dt}(I) = (\alpha \mathbf{f}_B + \beta \mathbf{f}_I + \gamma \mathbf{f}_C) \|\nabla \Phi(I)\|. \qquad (22)$$

This equation is composed of several « forces » acting on the contour, all in the direction of the normal. $\mathbf{f}_B$ is a boundary-based force that shrinks or expands the curve constrained by the curvature effect towards the object boundaries. $\mathbf{f}_I$ is an intensity-based force that moves the curve at the direction that creates interior regions with the desirable intansity properties. The decision about the curve position is based on the observed intensities, and the intensity-based object/ background. $\mathbf{f}_C$ is a visual consistency force that deforms the curve in the direction that minimizes the intensity error between the interior curve region and the object position at the previous frame. Besides, this force as well as the intensity-based force ensures the tracking operation by creating a consistent correspondence between the object position over the time. And $\{\alpha, \beta, \gamma\}$are positive normalized constants that balance their contribution.

The steady-state solution of the equation (22) and the geometric properties are estimated directly from the performed approximation showed in section 3. In our case the expression (13) deforms the initial curve. An approximation of (22) was performed with Hermes algorithm in [9]. This algorithm approximates curve evolution.

In Figure 7 we show the results from theory to practice. A low contrast image sequence (IR) is used to test our algorithm. The proposed algorithm works as follows : Given an initial curve and an image sequence from sequence, each object is associated to an intensity-based descriptor (it is estimated directly from the observed values). The algorithm creates correspondence between the current curve region and the corresponding object at the previous frame. Diffusion is made to propagate the initial curve. The curve is propagated towards one direction under a regularity constraint, σ^2. This term is very important since it ensures the regularity of the curve. The curve position is updated using expresion (17). Values from

diffusion and the correlated values from two frames are used for this task. Then, given the latest curve position, we update the reference frame and the intensity descriptor, and we proceed to the next frame. We have defined the weights to determine the modules contributions as follows $\{\alpha = \beta = \gamma = 1/3\}$.

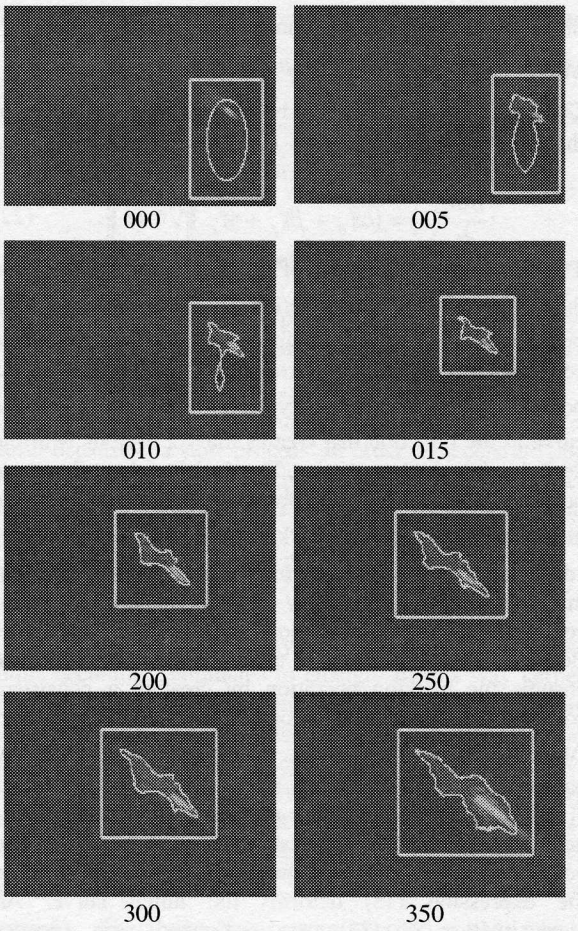

Figure 7 : *From top to bottom and left to right. Segmented video sequence (IR images), selected contributions* $\alpha = \beta = \gamma = 1/3$, *diffusion for propagating* $\sigma^2 = 1$. *Looking intensity values over 100.*

6. Application to pattern recognition

We now examine the adequacy of the standard scale-space paradigm for vision tasks which need « semantically meaningful » multiple scale descriptions. It is a simple and natural observation that maximal convex parts of objects determine visual parts and the more significant parts are recognized in higher abstraction levels. In this way current practice consists of performing Fourier series and to retain the first terms of the development as morphological attributes.

In this work the curve evolution allows to have an observed object in different abstraction levels.

One can describe a contour by defining its curvature in all point according to the curvilinear abscissa. This representation is a useful descriptor, since it has the profitable property of invariance with respect to basic similarity transformations, such as translation and rotation. Hence, the same shape appearing at a variety of positions and orientations, and possessing different starting points, would all yield the same set of descriptors.

Modifying locally the frontier of the region for determining the curvature. The curve $\Gamma'_{(x,y)}$, can be used such that to characterize a contour. Using curvature flow Fig. 8 shows three curve sets.

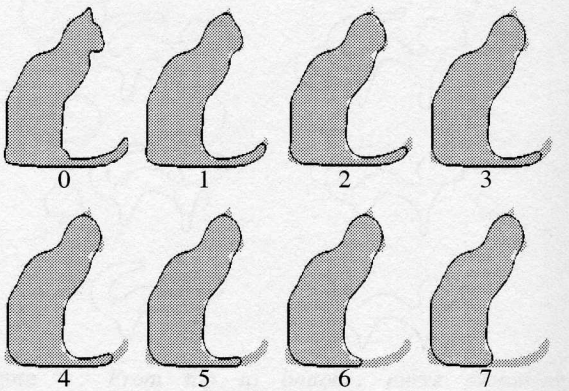

Figure 8 : *Curvature flow by the proposed sheme groupes* {0}, {1,2,3,4,5}, {6,7}.

7. Conclusion

We first have used classical definition of isotropic and anisotropic diffusion, then we have derived our performed method. As we have illustrated, the algorithm is very simple. That means proposed approximation requires simple calculs of linear filtering to perform curve evolution, thus numerical simulations may be developed very easily, and an explicit finite difference approach is posible. It was shown that an integration of advanced numerical techniques yield a computationally efficient algorithm that solves a geometric segmentation model. The numerical algorithm is consistent with the underlying continuous model.

Our anisotropic diffusion ideas were tested using a simple numerical scheme. In our performed approximation, the key idea has been an introduced auxiliary image. In this paper we have showed the profitable properties of performed anisotropic diffusion to be used as a mesure for shape descriptor.

Acknowledgements

The first two authors thank the CONACYT Scholarship Program of Mexico for their help and support.

References

[1] Witkin, A., *Scale-space filtering*. Int. Joint Conf. Artificial Intelligence, Karlsruhe, West Germany, 1983.

[2] Koenderink, J., *The structure of images*. Biol. Cybern. 50, 363-370, 1984.

[3] Babaud, J., Witkin, A., Baudin, and Duda, R., *Uniqueness of the gaussian kernel for scale-space filtering*. IEEE Trans. Pattern Anal. Machine Intell., PAMI-8, 1986.

[4] Yuille, A., Poggio, T., *Scaling theorems for zero crossings*. IEEE Trans. Pattern Anal. Machine Intell., PAMI-8, 1986.

[5] Hummel, A., Kimia, B., and Zucker, S., *Deblurring Gaussian blur*. Comput. Vision, Graphics, Image Processing 38,66-80, 1987.

[6] Perona, P., Malik, J., *Scale space and edge detection using anisotropic diffusion*. In Proc. IEEE Comput. Soc. Workshop Computer Vision, Miami, FL, 16-27, 1987.

[7] Kass, M., Witkin, A. et Terzopoulos, D. *Snakes :Active contour models*. In First International Conference on Computer Vision, p :259-268, London, June, 1987.

[8] Osher, S., Sethian, J., *Fronts propagating with curvature dependent speed : algorithms based on the hamilton-jacobi formulation*. Journal of Computational Physics. 79,12-49, 1988.

[9] N. Paraigios and R. Deriche. *Régions Actives Géodésiques et Courbes de Niveau pour l'Estimation du Mouvement et le Suivi d'Objets*, RFIA 2000, Paris, I :379-388, 2000.

[10] Marr, D., Hildreth, E., *Theory of edge detection* . In Proc. Roy. Soc. London B,207,182-217, 1980.

[11]Gage, M., Hamilton, R. S., *The heat equation shrinking convex plane curves*. J. of Differential Geometry. 23, 69-96, 1986.

[12]Alvarez, L., Guichard, F., Lions, P. L., Morel, J. M., *Axioms and fundamental equations of image processing*. Archi. For Rational Mechanics. 123(3),199-257, 1993.

[13]Sethian, J., *Level Set Methods*. Cambridge Univ. Press, 1996.

[14]Caselles, V., Kimmel, R, and Sapiro, G. *Geodesic active contours*. International Journal of Computer Vision, 22 :61-79, 1997.

[15] Venegas S. Rendon, J.M et Stamon G. ***Segmentation Spatio-temporelle en utilisant un front de propagation et champs de déplacement.*** Congres CORESA, novembre 2001, Dijon, France.